Increasing the Predictive Character of Spray Process Simulation by Multiphase Model Transitioning

Jochen Schütze*[1], Vinay Kumar Gupta[2], Pablo Aguado[3], Paul Hutcheson[4], Thomas Esch[5], Markus Braun[1]
[1]ANSYS Germany GmbH, D-64295 Darmstadt, Germany
[2]ANSYS Software Pvt. Ltd., Pune 411057, India
[3]ANSYS Iberia, E-28020 Madrid, Spain
[4]ANSYS UK, Ltd., Milton Park, Abingdon, Oxfordshire OX14 4RW, UK
[5]ANSYS Germany GmbH, D-83624 Otterfing, Germany
*Corresponding author: Jochen.Schuetze@ansys.com

Abstract

Liquid atomisation is an important operation in process industries, all kinds of liquid fuel combustion and several other contexts. The numerical simulation of such processes allows for their efficient optimisation as well as trouble-shooting. The aim of such simulations is to predict the complex physical phenomena in spray atomization based on material properties and first principles where possible and affordable.

The disintegration of a liquid jet, sheet or film usually happens in multiple steps: First, the contiguous liquid breaks into ligaments, which then split further into multiple droplets. The droplets can, depending on the surrounding gas flow, undergo further, so-called secondary break-up. Since the latter part only involves droplets in a surrounding gas flow, multiple semi-empirical (i.e. calibrated) models have been published for it that can be efficiently used in the Lagrangian formulation; this is a comparably “cheap” multiphase model approach that can be applied to relatively large flow simulation domains.

In contrast, the governing forces in the primary break-up are highly dependent on the individual atomizer design; a predictive simulation of this part of a spray is only possible using a “first principles” approach that resolves the shape and movement of the gas-liquid boundary in all detail. For that purpose, the Eulerian “Volume-of-Fluid” (VOF) multiphase simulation approach is recommended, which requires a high mesh resolution and small time steps. In order to achieve maximum modelling fidelity at minimum possible cost, the two approaches have been connected in the commercial general-purpose CFD code ANSYS Fluent by a model-transitioning mechanism. Its construction and some simulation results will be shown.

The use of dynamic solution-adaptive mesh refinement allows the user to accommodate the high-resolution mesh requirements for the VOF model at minimal computational effort. Still, small time steps need to be used for accurate interface tracking, which keeps the total computational cost considerable. It is therefore suggested, in addition to the model-transition, to split the spray simulation into two parts. The first part covers the in-nozzle flow and/or the near-nozzle dense spray region, which involves generating the droplets resulting from primary breakup and transferring them into the Lagrangian formulation. These droplets are injected into a second simulation that can be run much quicker because it only uses the Lagrangian approach for the dispersed multi-phase flow. This allows much larger simulation domains, and times, where the spray is considered dilute and secondary break-up can be modelled. The use of this cost-saving split approach will be demonstrated, including a further cost-saving step of reducing the computational effort for the Lagrangian droplets in the second part.

Keywords

CFD, Eulerian, VOF, Lagrangian, model transition, multi-scale modelling

Introduction

Liquid sprays are found in numerous industrial applications. In many situations, the purpose is to spread liquid over a large volume or surface area, e.g. in fire suppression, agriculture, cosmetic sprays or for various surface treatments such as cleaning, cooling or coating (spray painting). In other applications, the end purpose is liquid evaporation, e.g. in spray drying and cooling towers, or even a gaseous chemical reaction between the vapour and air, such as for liquid fuel combustion in internal combustion engines and gas turbines.

In all cases, the liquid atomization process creates large amounts of gas-liquid phase boundary. Usually, high liquid and/or gas momentum is used both to spread the liquid in space and to provide additional energy to overcome surface tension, which can be further aided by high levels of turbulence in the liquid.

In most spray processes, the droplet size distribution is paramount because it is linked to spray dispersion and evaporation, which play a key role in the overall success of the industrial application. For instance, small droplets enhance evaporation due to increased liquid surface per unit volume, leading to higher mixing quality [1]. Furthermore, small droplets typically lead to larger dispersion angle, improving the homogeneity of the mixture [2]. Conversely, large droplets have larger inertia and result in deeper spray penetration.

Numerical approach

Accurate control of the liquid atomization operation is very important for the success of the overall process, e.g. for achieving high efficiency and minimum pollutant exhaust from all kinds of liquid fuel combustion. Therefore, the optimisation of equipment and its operation using computational analysis is wide-spread and under continuous development.

For the numerical simulation of the multi-phase flows in liquid atomization, two fundamentally different approaches are generally in use: For any dilute spray region, in which discrete droplets occupy only a small percentage of the total volume, the “Euler-Lagrange” [3][4] formulation uses one set of Navier-Stokes equations for the gas flow (i.e. the “continuous phase”), while the liquid droplets (i.e. the “discrete phase”) are approximated by tracking their centroids in a Lagrangian frame of reference through that gas flow. The bi-directional exchange of mass, momentum, energy and potentially other quantities is accounted for by source terms in the Navier-Stokes equations for the gas phase, while the volume displacement caused by the presence of the droplets in the gas phase is often neglected. For dense spray regions, the “Euler-Euler” [5] approach is most appropriate. It treats multiple fluid phases similarly, accounting for each phase’s volume and the simple closure condition of a unity sum of all local volume fractions in every location. If a dispersed multi-phase flow is simulated on spatial scales much larger than the individual droplets, the idea of “interpenetrating continua” is employed, usually by solving a separate set of Navier-Stokes equations for every phase.

For stratified flows, as much as when even microscopic contiguous fluid bodies of the individual phases are resolved by the spatial (mesh) discretisation of the simulation, the “Euler-Euler” formulation can be reduced back to a single set of Navier-Stokes equations, extended just by a single transport equation for each phase to track its spatial distribution. Augmented by a suitable approach to account for surface tension and an explicit tracking of the phase boundaries, this “volume-of-fluid” (VOF) approach allows for high-fidelity, predictive simulations of the dense spray region with reduced computational cost.

Hybrid multi-phase flow simulation technique

The VOF approach requires a high spatial resolution in the fluid flow calculation in order to resolve the finest relevant liquid structures (ligaments and droplets) forming anywhere in the spray. Therefore, it is desirable to apply this technique only where it is needed. For the isolated droplets found in the dilute part of a spray, the “Euler-Lagrange” formulation can operate much more economically on a much coarser mesh.

Hybrid methods have been developed to combine the two approaches in a single simulation: The initial liquid flow is resolved on small spatial (and temporal) scales by the VOF approach; but where the spatial volume fraction field exhibits distinct, well-resolved near-spherical droplets, these are converted into Lagrangian particles, and at the same time the old VOF lump is removed. Herrmann [6] developed a refined level set method in order to capture the liquid/gas interface, and transitioned nearly spherical liquid structures within an upper size limit to the Lagrangian phase. The initial background meshes employed were very fine, up to 66 million cells to account for the flow gradients. Although good predictions of jet penetration were found, the level-set method used did not conserve mass.

Kim et al. [7] developed a similar hybrid method but with VOF instead of level-set, ensuring mass conservation. Mesh adaption was used to more efficiently capture the liquid/gas interface. Li and Soteriou [8][9] developed a hybrid method with coupled level-set, ensuring mass conservation but also a sharp interface. They demonstrated that using adaptive grid refinement, as well as mesh coarsening after droplet transition to the Lagrangian frame can offer huge cost savings. The mesh size after adaption was around 5 million cells. Ling et al. [10]’s hybrid model used VOF and DNS with extremely large meshes exceeding 4 billion cells, but addressed some important issues relating to hybrid techniques. A hybrid method has also been implemented in the commercial general-purpose CFD code ANSYS Fluent [11][12] and is used and extended in the present study.

The hybrid method provides most benefit when it is combined with dynamic solution-adaptive mesh refinement. The initial mesh is chosen to be coarse with few elements. Where higher spatial resolution is desired to resolve flow gradients and particularly the gas-liquid boundary, mesh elements are split into smaller ones based on relevant criteria. When a liquid structure is transported, the refined mesh region that it leaves can be coarsened again, while the new mesh area it travels into must be refined to sustain the spatial resolution of the respective liquid structure (**Figure 1**). Likewise, whenever a liquid "blob" is converted from the VOF formulation into a Lagrangian particle, the mesh refinement applied locally to resolve the shape of the liquid "blob" can be undone. That way, the Lagrangian simulation uses the coarse mesh and contributes very little to the overall computational cost.

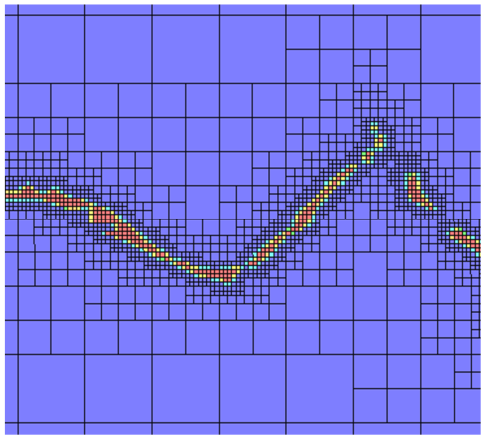

Figure 1. Visualisation of resolved liquid structures, travelling from left to right, and dynamic mesh adaption travelling with them.

Additional improvements

One purpose of spray simulations is usually the prediction of the droplet size distribution; but in many cases, even geometrical parameters like spray angle, penetration depth and even the spatial profile of the droplet size distribution is of interest. That requires the overall computational domain to be *much* larger than the dense spray region in which primary break-up occurs and the VOF approach is applied. This increases the cost of such simulations. Large domain extents mean larger cell counts.

More importantly, to predict for example the droplet size distribution far downstream, the spray must be simulated for a long period of time using a very small timesteps required at the gas-liquid interface. Therefore, it is desirable to be able to do the Euler-Lagrange simulation of the large dilute region of the spray at a separate, much larger time step. That can be achieved by splitting the simulation into two separate calculations, namely a hybrid VOF+Lagrangian simulation which is done in a computational domain that extends not much further than where only Lagrangian droplets cross. Information about all these droplets is then transferred into a separate calculation that only uses the Euler-Lagrange formulation, on a coarser mesh, and with time steps that are larger by potentially an even greater factor, because there is no longer a gas/liquid boundary to refine in the mesh.

Two facts need to be handled now: First, the total simulated time covered by an affordable VOF calculation of the primary break-up will be considerably shorter than that covered by the Euler-Lagrange calculation. The suggested resolution is to assume that the flow in the dense spray region reaches a quasi-steady state quickly: The characteristics of the time-resolved data that are recorded for the droplets produced by the primary break-up will, on average, become constant. Therefore, a suitable part of the exported data, corresponding to a time interval during which the quasi-steady state prevailed, can be used repetitively to fill larger amounts of time.

The other aspect to consider is the total number of Lagrangian particles: Usually, in practical spray simulations using the Euler-Lagrange approach, a reduced number of numerical *"parcels"* is used, each of which represents an arbitrary number of *identical* physical *particles*. All effects on the Lagrangian object are determined using the properties of a single physical particle, but effects on the Eulerian continuous phase are multiplied by the number of all the physical particles that are represented by the single numerical *"parcel"* object.

The VOF simulation is intended to capture the true number of physical *particles* produced by the primary break-up, at least down to the mesh resolution employed. The simulation detects distinct, isolated droplets in the VOF solution and converts them into Lagrangian particles. A software routine has been implemented to process all particles that have been converted and reduces the amount of data by reapplying the concept of *"parcels"* in a way that conserves the droplet count and total mass represented by a smaller number of particle *"parcels"*.

The remainder of this paper will first explain in more detail the approaches taken when these new software capabilities were created within the framework of the commercial general-purpose CFD program ANSYS Fluent; after that, successful use of the capabilities will be demonstrated on a few examples. An outlook on further work to be done will be given at the end.

Models and implementation

In this section, we will describe the components of the commercial general-purpose CFD program that were used for the simulations presented below; in addition, for those components that were newly implemented to tackle the problem described above, some details about their formulation will be discussed. For details about the pre-existing features in ANSYS Fluent, cf. the user documentation [13] and references cited therein.

Eulerian volume-of-fluid (VOF) method

For the VOF simulation, a single set of Navier-Stokes equations is solved in each mesh cell. In cells that are filled partly with either of the two fluids (gas and liquid), material properties are averaged by volume-weighting. Explicit tracking of the local volume fraction is used by way of the "geometric reconstruction" interface-tracking scheme in ANSYS Fluent, which is a piecewise-linear interface construction (PLIC) method [5].

During the explicit interface tracking, a global Courant number is calculated based on the global time step, the local cell volume and the volume flow rates entering the cell. If that global Courant number for the interface tracking exceeds a value of 0.25, sub-time steps are done for the volume fraction calculation such that the local Courant number in each step is no larger than this value. This way, decent accuracy can be maintained in the calculation of the interface movement despite the piecewise-linear geometric simplification of the morphology of the phase boundary.

Surface tension effects are included using the Continuum Surface Force (CSF) model as proposed by Brackbill et al. [14]. This, together with the explicit interface tracking, was chosen from the options provided by ANSYS Fluent because this choice provided good representation of surface tension forces without the additional numerical effort that would have been required for coupling a level-set transport equation to the straight-forward VOF formulation.

Dynamic solution-adaptive mesh refinement

In order to limit the total computational effort to the minimum necessary, the initial mesh is chosen coarse and solution-adaptive mesh refinement is applied where the gas-liquid boundary is, i.e. where the local liquid volume fraction is between 0 (zero) and 1 (one). As such, this approach ensures high mesh resolution exactly at the location of the phase boundary. (Cf. **Figure 1**) As the phase boundary moves, it will very soon leave the fully refined mesh cells, which must be avoided, because coarser cells mean reduced resolution of the interface morphology, and non-uniform cell sizes along the interface can impair the accuracy of the surface tension modelling. There are two solution-adaptive mesh refinement algorithms in Fluent, the default hanging-node adaption and PUMA (polyhedral unstructured mesh adaption) which can also refine polyhedral cells. The default was chosen since no polyhedral cells existed in the baseline mesh.

Every pass through the solution-adaptive mesh refinement algorithm means additional computational effort, so it is desirable to limit the frequency at which such adaption passes are needed. Therefore, multiple cell layers *around* the gas-liquid interface should be refined. That is achieved most effectively by using the spatial second derivative, or curvature, of the volume fraction field as a simple means to mark cells in multiple layers around the resolved phase boundary: Wherever the magnitude of that "curvature" is larger than zero, cells are refined / prevented from being coarsened, and only where it is zero, refined cells are coarsened. This way, even if the phase boundary crosses an entire cell layer per time step, mesh adaption every other time step is sufficient to always keep the phase boundary well inside the fully refined region.

For turbulence modelling, the "SST-SBES" hybrid RANS-LES turbulence model was chosen [15]. It can adapt itself to the mesh resolution so that in fine-mesh regions, it operates in an LES mode, while the full RANS model is active where the mesh is too coarse to resolve the majority of the turbulent flow structures. In close vicinity to walls, the "WMLES" sub-grid scale LES model, embedded in the SBES framework, provides the appropriate wall boundary layer modelling in the LES mode. The aggressive use of local mesh refinement will have an impact on the turbulence modelling, since LES filtering depends on the mesh resolution. The impact e.g. on the droplet size distribution is yet to be investigated in detail. It is expected to depend much on the relevant mechanisms in drop formation in the individual flow, so general advice will remain vague.

VOF-to-Lagrangian model transition

For the VOF-to-Lagrangian conversion, the VOF liquid volume fraction field is searched, at regular intervals (e.g. every 50th time step), for contiguous bodies of liquid that are surrounded by pure gas (zero liquid volume fraction). Proper candidates have a core of "pure" liquid (volume fraction at least close to unity), but depending on mesh resolution and time step size, a user may choose to allow some areas of diffuse liquid (volume fraction less than unity) to form e.g. in flow directions that are not of interest. Such "diffuse lumps" can be removed from the solution to stop them from triggering local mesh refinement. The proper candidate liquid "lumps" are then characterised and elected for conversion by multiple criteria: (1) The volume must fall into a user-specified range, and (2) the shape must be close to spherical by user-specified tolerances.

For the characterisation of the shape, two measures for the deviation from a perfect sphere have been derived. Both are calculated from the lump's centre of gravity and an averaging over all computational cells in the periphery

of the lump, i.e. those that are part of the lump (non-zero liquid volume fraction) but for which the liquid volume fraction is lower than in the core:

For the first measure, the distance between the centre of gravity and the reconstructed linear piece of lump surface is calculated for each of the periphery cells, and the standard deviation of all these "radius" values is determined. (Cf. **Figure 2**) Normalising that by the radius of a volume-equivalent sphere, a quantity is obtained that is 0 for a perfect sphere and non-zero (with no upper limit) otherwise.

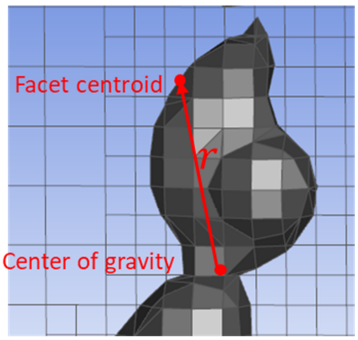

Figure 2. Calculation of "asphericity" by normalised "radius" standard deviation.

For the other "asphericity" measure, dot products of the "radius" (from the centre of gravity to the individual periphery cell) and the normal vector of the reconstructed linear piece of lump surface (both vectors normalised) are calculated for all periphery cells. The arithmetic average of all these values is 1 for a perfect sphere and (close to) 0 for highly non-spherical shapes. (Cf. **Figure 3**)

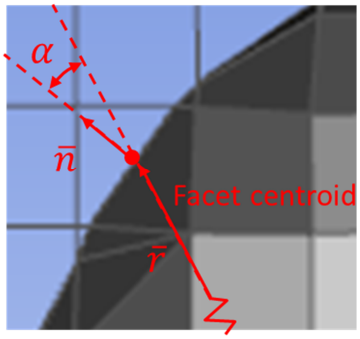

Figure 3. Calculation of "asphericity" by "radius—face orthogonality"

The "normalised radius standard deviation" approach distinguishes sensitively between perfect spheres and slightly deformed shapes that are still relatively close to the perfect sphere; in contrast, the "radius—face orthogonality" approach is more suited for discriminating drastically non-spherical shapes from those that are relatively close to the perfect sphere. (Cf. **Figure 4**)

Lagrangian particle tracking

For the dilute part of liquid sprays, the Lagrangian formulation (tracking individual or representative droplets) is used [16]. Because of the small volume fraction that is, on average, filled by the droplets, this approach for modelling the dispersed multi-phase flow is simplified by neglecting the volume displacement caused by droplets in the continuous gas phase. Therefore, during the model-transitioning from VOF liquid to Lagrangian particles, their volume is lost. For the sake of numerical robustness, this is compensated by replacing the VOF liquid by an equal amount (by volume) of gas of the same velocity & temperature.

When a liquid "lump" is to be converted into a Lagrangian particle, the mesh refinement that was applied to resolve the morphology of the VOF gas-liquid boundary is undone, i.e. the mesh is coarsened back to its initial form. This is, unless coarsening would result in a conflict with other mesh adaption requirements. Because of this and other reasons, it is not unlikely that a Lagrangian particle that is formed from a VOF liquid lump represents a single physical liquid droplet that is much larger (by volume) than the mesh cell in which it is placed. That is not found to be a problem from a robustness point of view; but if for example a Lagrangian droplet evaporates quickly in a hot gas, it may cause strong mass & enthalpy source terms in the cell with adverse effects on convergence and robustness of the solution of the Eulerian transport equations for the continuous gas phase. To avoid such issues, Lagrangian particles that exceed the cell volume by a configurable factor can be split into numerical parcels, one

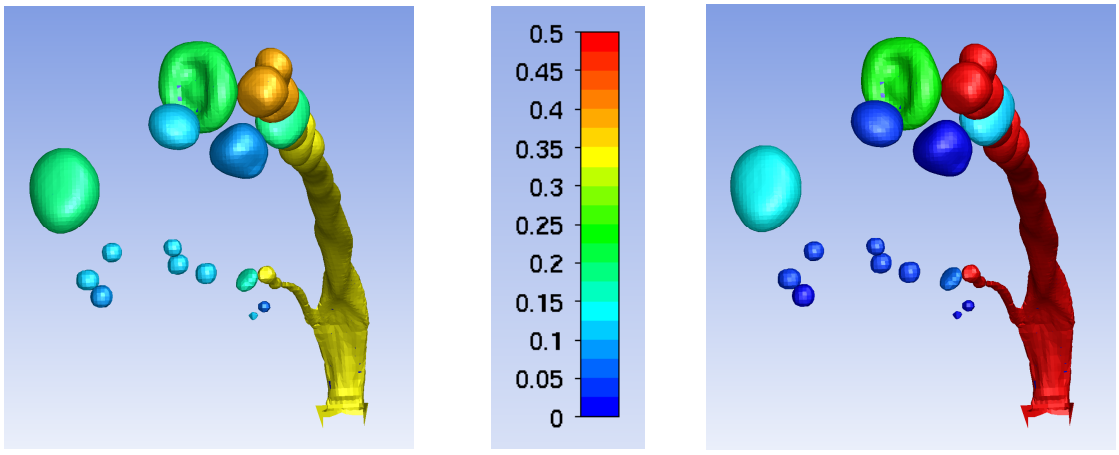

Figure 4. *Left:* Asphericity by normalised "radius" standard deviation. *Right:* Asphericity by radius—face orthogonality

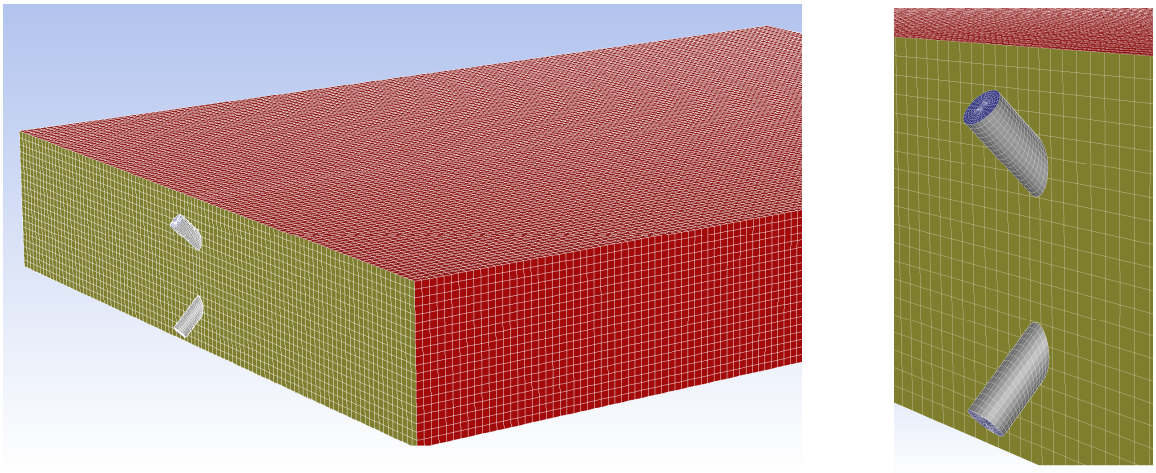

Figure 5. *Left:* Visualisation of the computational domain and initial mesh resolution. *Right:* Detail of the inlet piping.

per cell that is covered by the shape of the VOF liquid lump, each representing the part of the liquid droplet that is equivalent to the cell's volume.

Data transfer and data reduction

During the simulation, whenever a VOF liquid lump is transitioned to the Lagrangian formulation, a record of its properties is written to a file. The information written includes the location and the simulated time. Based on these, an independent flow calculation that only uses the Lagrangian method for modelling the multi-phase flow can "inject" Lagrangian particles at the appropriate times and locations. This independent calculation can cover larger periods of time, for which a certain time interval from the written records can be repeated infinitely, assuming a quasi-steady state. On the larger temporal and spatial scales of the independent simulation, it may be desirable to reintroduce the traditional parcel concept, where a single parcel represents multiple particles of similar properties.

The parcel concept is applied even to the written record of all particles created from VOF liquid lumps: Conservative data reduction is applied to these data by (1) searching for pairs or groups of entries that are similar, by configurable tolerances, in all properties (location, size, velocity, temperature, time of conversion…) and (2) combining those into a single parcel that represents a number of (identical) particles of the averaged properties. Both the number and the mass of the particle population represented by those parcels conserve the particle count and mass of the initial particles.

Flexible control of the tolerances that are used to identify those pairs or groups of particle entries is achieved by dividing the total range of each variable (droplet size, position coordinates, time of conversion etc.) into an adjustable number of intervals (scaled linearly or logarithmically). As this is done for all variables simultaneously, it forms a multi-dimensional state-space of all the variables by which every entry is uniquely characterised. Where multiple entries occupy the same interval with respect to every variable, they can be combined into a single parcel to represent their number of (identical) particles of their average properties.

Steady-state representation

If the time of conversion is dropped from the list of particle variables considered in this data reduction operation, the data can be reduced into a steady-state representation: Like before, entries occupying the same N x N matrix cell in the discretised multi-dimensional state-space are averaged for all variables, but the "number-in-parcel" is replaced by a *frequency* at which physical particles of the averaged properties would be released from the individual location to best represent the original population of particles created over time by the model transition.

Such a steady-state representation can be used in a transient multi-phase flow simulation and allows even more flexible control of the number of the Lagrangian numerical particle "parcels" injected: Whilst the standard method is to inject one numerical parcel per time step for each location listed in the file, it is possible to control injection times automatically such that every particle parcel represents a specified *number* or *mass* of particles.

Results and discussion

Double-impinging jets example

For verification and demonstration purposes, a simple configuration of two water jets, with an average velocity of 100 m/s and 3 mm in diameter, impinging on each other at an angle of 90°, was considered. A symmetrical flat fan forms in the half-angle plane between the jets, forms instabilities and breaks down into (initial) droplets.

For the calculation, an initial mesh of 270,680 hexahedral cells in the brick-shaped flow domain of 205 mm length, 150 mm width and 29 mm height (**Figure 5**). With hanging-node solution-adaptive mesh refinement, the total cell count stabilised between 10 and 11 million cells. The uniform cell edge length in the initial mesh was almost 1.5 mm; the fully refined cells (4 levels of hanging-node refinement) had a cell edge length of approx. 95 µm. The time step size was 0.2 µs, maximum Courant numbers detected in the explicit interface tracking were constantly at almost 1.1 while the convective Courant numbers calculated from face volume flow rates and cell volumes ranged between 0 and 0.5, at maximum local velocity values close to 200 m/s.

Figure 6 shows a perspective view of the liquid flow morphology, captured as VOF liquid (grey) and Lagrangian particles (coloured by their size). During 2 ms of simulated time, 2.77 g of water left the nozzles into the domain. After that time interval, the domain contained 1.07 g of VOF liquid, and the accumulated Lagrangian particle data indicated that a total of 1.69 g had been converted, which adds to a sum of 2.76 g, i.e. within round-off errors, all mass was conserved.

Each time the VOF solution was searched for detached liquid lumps to convert, firstly only those lumps were considered whose volume was smaller than that of a sphere 100 µm in diameter. These were converted regardless of their shape, because the mesh (minimum cell size allowed of approx. 95 µm) was not able to reasonably resolve them anyway. Almost 22,000 such lumps were detected. After that, all lumps up to the volume of a 2 mm-sphere were converted whose shape did not deviate much from spherical. A total of 105,700 lumps was converted, all between 100 µm and 900 µm volume-equivalent sphere diameter, with a Sauter mean diameter of 360 µm. Finally, 400 lumps were found whose interface had been smeared by numerical diffusion such that they did not contain any cell with a volume fraction of 0.1 or above. More than 99% of these lumps had volumes corresponding to spheres less than 70 µm in diameter, i.e. much below the finest mesh resolution.

The entire simulation, including the generation of pictures every 25 time-steps for smooth animations, took 6 days on 166 Intel Xeon X5670 CPU cores at 2.9 GHz, distributed over 13 dual-socket machines connected with Infiniband. (No investigation was made into the parallel scaling, i.e. how much longer it would have taken on fewer cores.) As described above, during the simulation, information about all the lumps detected and converted was exported. These data were then used to inject particles in a purely Lagrangian simulation. This one was run on 19 of the above cores (distributed across two machines) on the initial 270,680-cell mesh, without any mesh refinement, and with 5 µs time steps, which took an overall wall-clock time of 50 minutes – again including time for exporting pictures at the same intervals of simulated time, i.e. now *every* time step. A visualisation of the result is shown in **Figure 6** to the right. It is obvious that the spray pattern captured in the Lagrangian formulation evolves very similarly to the hybrid VOF-Lagrangian calculation. This is the basis for spray simulations over larger scales in space and time.

Conclusions

By implementing a VOF-to-Lagrangian model transition mechanism, a hybrid Eulerian VOF—Lagrangian modelling approach was implemented in the commercial general-purpose CFD code ANSYS Fluent. It gives the simulation of

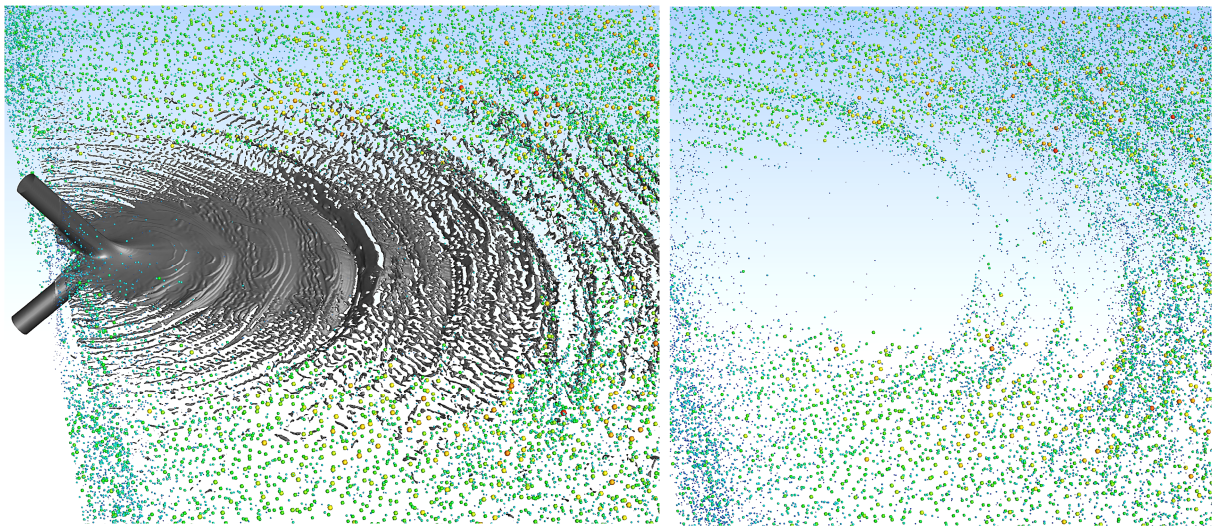

Figure 6. *Left:* Perspective view of the double-impinging jets configuration; the VOF liquid surface appears in grey shades, Lagrangian particles in colours depending on their size. Water/air at standard conditions; liquid jets 3 mm in diameter and 100 m/s velocity. *Right:* Result of the purely Lagrangian calculation using the lump conversion records from the VOF run.

primary break-up the predictive character of the independence of e.g. atomizer models that are established and calibrated for individual injector types, and still uses the much more economic Lagrangian formulation to cover larger scales in time and space. This is fully achieved by uncoupling the large-scale Lagrangian simulation from the high-resolution VOF calculation for the primary break-up. On a first example application, the feasibility of applying this to industrially relevant spray processes has been demonstrated.

Outlook

The VOF-Lagrangian model transition does not involve any mathematical modelling, it just ties together two well-established multi-phase flow modelling techniques. Still, it is desirable to further validate the applicability of the overall approach to different industrially relevant types of spray processes. This is an important topic for near-future activities.

In addition, there is room for further improvement in the initialisation of Lagrangian particles created: Secondary break-up models that are commonly used in Lagrangian simulations will likely benefit from careful initialisation based on the VOF liquid lump's shape & rate of deformation as well as age of liquid (since entering the domain from the Eulerian inlet boundary) and time since detachment ("pinch-off" of the drop from the contiguous liquid jet or sheet).

Finally, as of the time of writing, no proper handling is applied yet in the event that a Lagrangian particle collides with any mesh-resolved VOF liquid. This can pose problems in case a secondary break-up model is applied to the Lagrangian particle, and the implementation of a proper resolution is the subject of ongoing efforts.

Acknowledgements

The authors wish to express their special thanks to their colleagues Vivek Kumar, for invaluable pioneering work, as well as Muhammad Sami, for testing and feed-back, and Amine Ben Hadj-Ali, for many fruitful discussions.

References

[1] Moon, S. et al., 2007, J. Phys.: Conf. Ser., 85, 012004.

[2] Hespel, C., Blaisot, J.-B., Margot, X., Patouna, S., Cessou, A., Lecordier, B., 2010, THIESEL 2010 Conference on Thermo- and Fluid Dynamic Processes in Diesel Engines.

[3] Reitz, R. D., 1987, Atomization and Spray Technology, 3, pp. 309-337.

[4] Schmidt, D., 2006, International Journal Numerical Methods Fluids, 52, pp. 843-865.

[5] Youngs, D. L., 1982, "Numerical Methods for Fluid Dynamics", pp. 785-807.

[6] Herrmann, M., 2010, J. Eng. Gas Turb. Power, 132, 6, pp. 451-466.

[7] Kim, D., Ham, F., Le, H., Herrmann, M., Li, X., Soteriou, C., Kim, W., May 2014, ILASS Americas 26th Annual Conference on Liquid Atomization and Spray Systems.

[8] Li, X., Soteriou, M., May 2014, ILASS Americas 26th Annual Conference on Liquid Atomization and Spray Systems.

[9] Li, X., Soteriou, M., Jan. 4.-8. 2016, 54th AIAA Aerospace Sciences Meeting.

[10] Ling, Y., Zaleski, S., Scardovelli, R., 2015, Int. J. Multiphase Flow, 76, pp. 122-143.

[11] Sonawane, R., Kumar, V., Nakod, P., Dec. 7.-8. 2017, ASME 2017 Gas Turbine India Conference.

[12] Schütze, J., Kumar, V., Braun, M., Sami, M., 2018, ICLASS 2018: 14th International Conference on Liquid Atomization and Spray Systems.

[13] ANSYS, Inc., 2019, ANSYS Fluent Theory Guide.

[14] Brackbill, J. U., Kothe, D. B., Zemach, C., 1992, J. Comp. Phys., 100, 2, pp. 335-354.